Journal of the European Ceramic Society 15 (1995) 455–461

0955-2219/95/$9.50

0955-2219(95)00003-8

Thermal Shock Resistance of Nextel/Silica–Zirconia Ceramic-Matrix Composites Manufactured by Freeze-Gelation

A. Twitty,[b] R. S Russell-Floyd,[c] R. G. Cooke & B. Harris[a]

School of Materials Science, University of Bath, Bath BA2 7AY, UK

(Received 18 October 1993; received in revised form 24 November 1994; accepted 12 December 1994)

Abstract

Ceramic-matrix composites consisting of a silica–zirconia matrix reinforced by 25% by volume continuous Nextel alumino–silicate fibres have been manufactured by a sol–gel route incorporating freeze-gelation and subjected to thermal shock by water quenching from temperatures up to 800°C. Although it was demonstrated that the Nextel fibres exhibited significant degradation of properties during composite processing, they still had a significant reinforcing effect. The material showed a critical temperature of approximately 550°C, below which it was unaffected by water quenching. Above this level there was a 40 and 50% step reduction in modulus and strength respectively. Acoustic emission monitoring showed a significant difference in materials subject to quenching from beyond the critical temperature. There was a lower initial yet higher final AE event rate for a monotonically increasing flexural load, and a bimodal amplitude distribution. This indicated that the material responds in general terms in the manner corresponding to the well-known Hasselmann model of thermal shock of monolithic ceramics, but the presence of fibres appears to improve the thermal shock resistance by raising the predicted critical temperature somewhat.

1 Introduction

The sol–gel process offers the possibility of manufacturing a wide range of ceramic-matrix composites (CMCs) in near-net shape and size by the use of techniques familiar in the processing of polymer-based composites and without the need for such costly manufacturing procedures as are commonly required to process conventional ceramics or CMCs.[1,2] The properties of such composites are more modest than those normally required for aerospace and other high-performance applications, but there are many uses for ceramics in general engineering for which the properties available in sol–gel CMCs are adequate, provided some measure of toughness and resistance to thermal shock can be incorporated. One of the difficulties with any CMC system is that, during either manufacture or subsequent service at elevated temperature, interfacial interactions can lead to deterioration of the fibres so that the full potential strength of the system cannot be realised in practice. An advantage of the sol–gel route in this respect is that it permits lower final firing temperatures and, therefore, the possibility of restraining such adverse reactions during processing. One of the systems that we have been studying as part of a wider program on CMCs manufactured by the sol–gel route is a composite consisting of a silica-based matrix reinforced with Nextel mullite fibres. In this paper we describe a series of experiments to investigate the resistance of this material to water quenching from temperatures up to 800°C.

2 Material

The reinforcing fibre was Nextel 440, manufactured by the 3M Company, a mullite material consisting of 70 wt% alumina, 28 wt% silica and 2 wt% B_2O_3. The manufacturer gives values of 186 GPa for Young's modulus and 2·1 GPa for the tensile strength of this fibre. The matrix ceramic is a silica–zirconia compound prepared from a mixture of Syton HT50, an aqueous sol containing 50 wt% of colloidal SiO_2 and 50 wt% of water, manu-

[a]To whom correspondence should be addressed.
[b]Present address: Johnson Matthey Technology Centre, Sonning Common, Reading, Berks, UK.
[c]Deceased.

factured by Monsanto, and Zircosil, consisting of 61 wt% of ZrO_2, 36 wt% of SiO_2, and small quantities of Al_2O_3, HfO_2, TiO_2, and Fe_2O_3, manufactured by Cookson Minerals.

The matrix components were mixed with a high-shear disperser and the resulting sol was used in a filament-winding process to produce flat plates of unidirectional impregnated sheet. These sheets were then wet-pressed between stainless steel platens to consolidate the windings and to produce plates approximately 100 × 100 mm × 5 mm. The pressed plates were then freeze-gelled by cooling rapidly in liquid nitrogen, following which they were warmed slowly to ambient temperature to produce a porous solid that could be handled. After drying to remove the excess residual water from the sol, the plates were infiltrated three times with Syton D30 silica sol, drying between infiltrations, and then sintered at 950°C for one hour. The sintered plates were then twice re-infiltrated, following which they were cut into 10 mm wide test pieces with a water-cooled diamond saw to provide unidirectionally reinforced composite samples. The cut samples were then re-infiltrated a further three times and finally sintered again at 500°C for 90 min. Three separate batches of the composite were prepared by this procedure with identical processing conditions. Image analysis of composite cross-sections gave average values of the fibre volume fraction, V_f, of 0·26, 0·23 and 0·28, respectively for the batches identified as A, B and C. The fibre distribution was reasonably uniform the final level of matrix porosity was about 30 vol%.

3 Testing Procedures

Mechanical strength and stiffness were determined by flexural testing in three-point bending with a span-to-depth ratio of 16:1 at an Instron crosshead displacement speed of 1 mm.min^{-1}. An indication of the relative toughnesses of the samples was also obtained from the area under the flexural load–deflexion curve. And in order to establish the inherent (undamaged) stiffness of the material, dynamic stiffness values were obtained by time-of-flight and density measurements. All test results reported in this paper are the averages of at least five individual tests.

Thermal shock experiments were carried out by heating samples to different temperatures in the range 200 to 800°C, soaking for 20 min to establish thermal equilibrium, and then quenching into water at 20°C. After the samples were completely cooled, they were furnace dried at 60°C for 24 h. Five samples quenched from each temperature were then used for the determination of the mechanical properties in the quenched condition, as described above. The samples used for these experiments were all from batches A and B. For comparison purposes, a group of samples from batch C were subjected to the same thermal cycle but were slow-cooled from the upper temperature rather than quenched, and samples from batches B and C were heated rapidly from room temperature to the same maximum temperatures as used for the quenching experiments. These samples were also mechanically tested as described above.

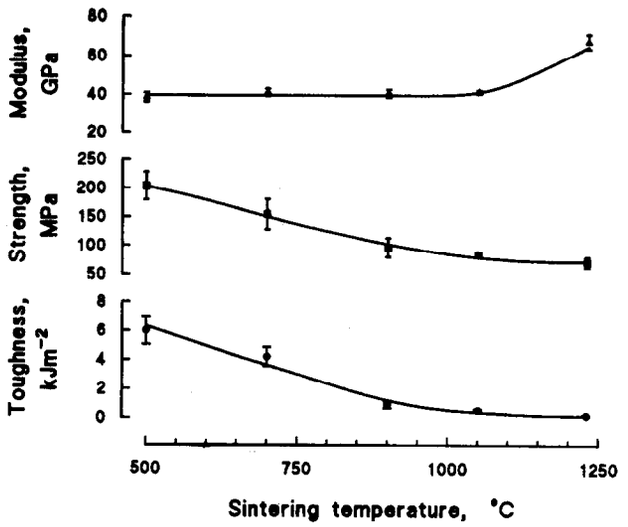

Fig. 1. The effect of raising the sintering temperature on the mechanical properties of freeze-gelled Nextel/silica–zirconia ceramic-matrix composites.

Many of the mechanical tests carried out in this work were accompanied by the monitoring of acoustic emissions. A Marandy MR1004 25-channel amplitude distribution system was used to record emissions received through a PAC U30D-174 PZT transducer and an AECL 2100/pa 60dB preamplifier. The AE data were processed by custom-written software and analysed by means of a conventional spread-sheet program.

The thermal expansion characteristics of the composite over the range 20°C to 650°C were determined in a silica tube dilatometer.

4 Experimental Results

The mechanical properties of the three batches of unidirectional composite after manufacture are given in Table 1.

It can be seen that the strengths and stiffnesses of the three batches of material (which were made by identical procedures, as described earlier) are to all intents and purposes identical, as would be expected. The dynamic stiffness is significantly higher than the flexural modulus measured from

Table 1. Mechanical properties of as-manufactured Nextel/silica–zirconia composite*

Batch	*Fiber volume fraction* V_f	*Dynamic modulus, GPa*	*Flexural modulus, GPa*	*Flexural strength, MPa*	*Work of fracture,* Jm^{-2}
A	0·26 ± 0·01	40 ± 2	31 ± 6	79 ± 18	477 ± 155
B	0·23 ± 0·01	40 ± 1	36 ± 2	84 ± 14	502 ± 111
C	0·28 ± 0·01	44 ± 1	41 ± 4	83 ± 13	871 ± 256

*Errors cited are standard deviations: five test results for each value cited.

the slope of the load–deflexion curve because it effectively assesses the response of an undamaged structure, whereas the mechanical modulus is not a simple elastic property in CMCs, since it inevitably includes some effect of the loss of stiffness due to cracking during loading. It is curious to note, however, that the nominal work of fracture of batch C is almost 50% greater than that of batches A and B. There is little evidence of any kind to explain this difference, the fibre content being only marginally higher, and there being no observable difference in microstructure. The higher fracture work was clearly seen to be the result of a different fracture mode in material of batch C which exhibited a considerable amount of delamination during fracture, whereas the failures of the other two batches were by completely transverse fracture. This difference is also reflected in the higher value of the mechanical flexural modulus. The only possible difference in the processing conditions between batches might be the level of pressure applied during the wet-pressing operation to consolidate the filament-wound material prior to freeze-gelation. This pressure was not controlled, since we had not expected that it would have a significant effect on the properties of the finished composite: this could prove to have been an important processing parameter, however.

On the basis of the manufacturer's value for the fibre stiffness, 186 GPa, the measured composite (dynamic) modulus appears to reflect, almost exactly, a fibre-only contribution (i.e. ¼ of 186 ≈ 46 GPa). In a CMC, this is unlikely, even when the matrix is porous, as in the present case. Earlier work on similar systems[2] suggests that the intrinsic stiffness, E_0, of a dense sol–gel silica matrix may be of the order of 70 GPa, and for a sample with a volume fractional porosity, p, of 0·3 a reasonable value, given by the relationship:

$$E = E_0 \exp(-4p)$$

would be 21 GPa, making an expected composite stiffness of about 65 GPa, some 60% greater than the measured dynamic value. Similarly, a crude estimate of the expected composite strength, based on the manufacturer's figure for the fibre strength (in excess of 2 GPa) and ignoring any matrix contribution, gives a value of the order of 570 MPa, yet the measured strengths in Table 1 imply a fibre strength of the order of only 320 MPa. This enormous loss of strength appears to be a consequence of damage which occurs during processing. Experiments in which tows of the Nextel fibre were passed through the desizing process and then through the guide system through an empty sol bath, for example were found to have lost some 40% of their original bundle strength.[3] Tows of T300 carbon fibre similarly lost about 35% of their original strength during this part of the process. The measured bundle strength of a tow of about 2000 filaments of 11 μm diameter was 198 MPa. Assuming a Weibull modulus of the order of 10, and therefore a bundle strength of the order of 60% of the individual filament strength, a bundle strength of 198 MPa translates to a filament strength of about 330 MPa. Without any more detailed scientific basis for accounting for the difference in gauge lengths in the bundle tests (90 mm) and effective 'gauge length' *in situ* in the composite, this agreement with the measured strength in Table 1 is more than adequate.

As the sintering temperature is raised from 500°C to 950°C the strength declines by about 60%, as shown in Fig. 1, while the modulus (and also the density) increase as consolidation is enhanced. The 950°C sintering temperature was chosen for these experiments to permit the thermal shock experiments to be carried out to a maximum quenching temperature of 800°C. Microstructural evidence, such as that shown in Fig. 2, clearly indicates that significant fibre/matrix interaction does indeed occur during the sintering stage, but it appears that this is not the only

Fig. 2. Electron micrograph showing fibre/matrix interaction in a freeze-gelled Nextel/silica–zirconia ceramic-matrix composite during sintering at 500°C following infiltration.

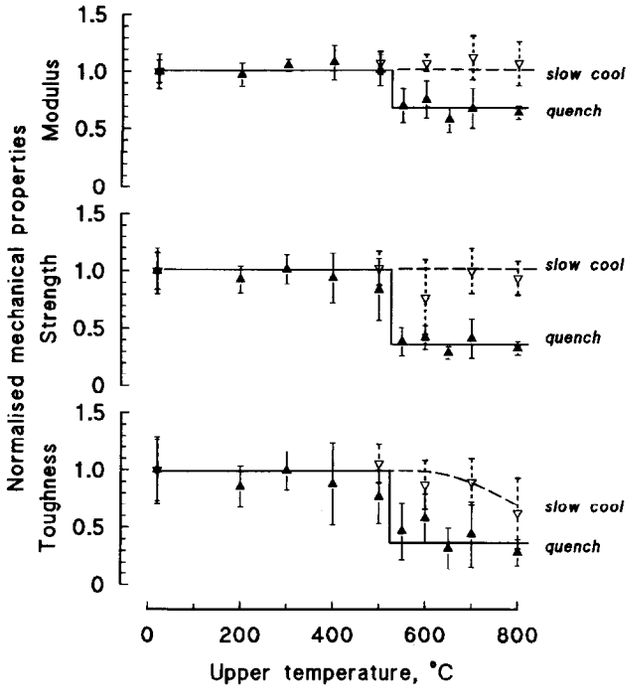

Fig. 3. The effect of slow and rapid cooling on the mechanical properties of freeze-gelled Nextel/silica–zirconia ceramic-matrix composites. The open symbols represent samples of batches A and B (pooled data) water-quenched from the stated soak temperature, while the solid symbols represent samples from batch C slow cooled from the stated temperature. Each point for batches A/B is the mean of ten individual tests, and each point for batch C is the mean of five tests: the error bars are standard deviations.

source of damage. A important secondary advantage of the freeze-gelation process is that the dried but unsintered product has considerable strength as a result of the molecular forces involved in the sol-gel transformation, a situation paralleled to some extent in the 'setting' of the tobermorite gel in cement, and this has important implications for the handling and shaping of pre-sintered products. Thus, we have found that the freeze-gelled material can be tensile tested in the unsintered state after vacuum-drying at a temperature slightly above ambient, followed by further infiltration (but no sintering) to yield a strength of only 155 ± 5 MPa, and this strength falls to 127 ± 7 MPa after sintering at only 500°C. Clearly, then, the Nextel fibre loses most of its reinforcing potential as a result of either corrosion in the sol bath, or abrasion at some stage during the consolidation process. It appears, therefore, that this fibre cannot be considered as a serious contender for use in CMCs manufactured by this process.

The axial coefficient of thermal expansion (CTE) varies strongly with temperature over the range studied, rising from about $2{\cdot}8 \times 10^{-6}(°C)^{-1}$ at ambient temperature to about $6 \times 10^{-6}(°C)^{-1}$ at about 500°C. The variation is approximately linear in temperature, being given by the relationship:

$$\alpha = 2{\cdot}69 \times 10^{-6} + 6{\cdot}44 \times 10^{-9}\, T \qquad (1)$$

The room-temperature CTE of the Nextel fibre is quoted by the manufacturer as $5 \times 10^{-6}(°C)^{-1}$. We have no measured value for the unreinforced matrix material appropriate to its condition in the sol-gel composite, but a value of about $2 \times 10^{-6}(°C)^{-1}$ would, on a crude rule-of-mixtures basis, give the observed CTE of about $2{\cdot}8 \times 10^{-6}(°C)^{-1}$ for the unidirectional composite.

4.1 Thermal shock results

The effects of water quenching on the properties of the composites of batches A and B (filled triangles) are shown in Fig 3. In view of the similarity of properties of batches A and B shown in Table 1, the data for these two batches have been pooled. The A/B data points in Fig. 3 are therefore means of ten individual tests and the error bars represent the standard deviations. Each set of results is normalised with respect to the appropriate property of the as-manufactured composite (i.e. the values given in Table 1) for ease of comparison. It can be seen that the stiffness, strength and mechanical modulus all remain unaffected by quenching until the soaking temperature exceeds 500°C. Above this all three properties fall drastically in step functions to levels that are about 50% of the original values in the case of the strength and toughness, and 60–70% of the initial values for the stiffness. In order to show that it is the thermal shock that is responsible for this sudden loss in properties, samples of batch C were subjected to the same heating and soaking procedure, but were then slow cooled in the furnace from the soak temperature. It can be seen that the strength and stiffness are unaltered by this treatment, but the toughness does change, falling more gradually beyond about 500°C to some 60 or 70% of the initial value. Table 1 shows that the original toughness of batch C was much higher than that of batches A and B, and the corresponding decline in toughness of the material of batches A and B as a result of slow cooling may well be more severe than that shown for batch C in Fig. 3.

As a further check on the role of the downquench, as opposed to other heating effects, in degrading the properties of the composite, a small group of samples was also subjected to the same temperature change by rapid heating up to the soaking temperature. These results are shown in Fig. 4, from which it is clear that the values of all three mechanical properties are substantially unchanged by either slow cooling or rapid heating from 800°C.

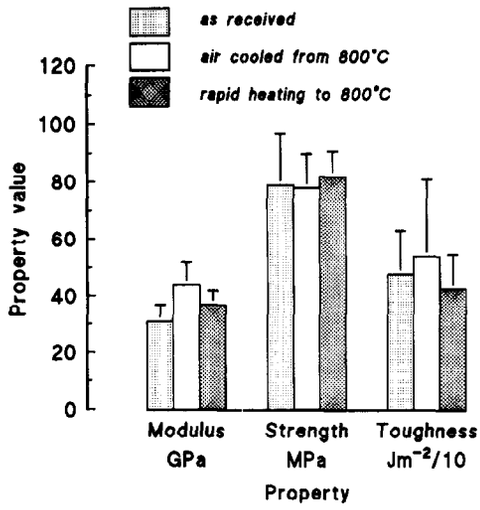

Fig. 4. Effects of slow cooling from 800°C and rapid heating to 800°C on the properties of the Nextel/silica–zirconia CMCs.

The changes in acoustic emission response from quenched and unquenched samples give some insight into the effect of the thermal shock on the damaged state of the material. Figure 5 shows the cumulative total number of AE events emitted by samples during flexural testing as a function of the soak temperature prior to quenching. The data points are the averages of five separate tests and the error bars are the standard deviations. It can be seen that in the as-manufactured state the total AE count is about 800 events, a low output for a unidirectional fibre composite material. There is little change in the total AE count for samples quenched from temperatures up to about 500°C (the slight depression between the as-manufactured level and the level at 500°C is probably not significant, given the variable character of these materials and the general nature of AE phenomena) but beyond 500°C the acoustic response increases markedly, reflecting the sudden deterioration in mechanical properties of samples quenched from above 500°C. Analysis of the amplitudes of the AE events which constitute the general pattern shown in this figure provides further information on the effects of the quench. Figure 6 shows the amplitude distribution histograms for samples loaded to fracture in bending in the as-manufactured state and after quenching from 800°C. These distributions are for the final stages of the two tests, with the samples nearing fracture, a method of AE analysis which emphasises changes in mechanisms by reducing the masking effect of the large numbers of events recorded in the early stages. The bars in the histogram therefore represent the numbers of events emitted during the last few seconds of a test which fall in the amplitude band defined by the amplitude channel number on the abscissa. The width of each amplitude bin is 2·4dB. A voltage of 10 mV at the amplitude sorter for channel 0 represents 10 μV at the transducer. The threshold in these tests was set at channel three to exclude extraneous signals, and hence the actual test threshold was 20·9 mV. In the un-quenched condition, the form of the distribution is roughly exponential, with no significant numbers of events having amplitudes above 832mV (channel 15), the normal kind of distribution found in many types of composite, including CMCs. By contrast, the distribution for the quenched sample shows three distinct features. Apart from the increase in the total event count already referred to, it is clear that there are also many events of much higher amplitude than those in the un-quenched sample, and the distribution has become bi-modal, with a peak at an amplitude of about 363mV (channel 13). This is indicative of the late onset of a different mode of damage, or the operation of an existing damage mode at much higher energy levels.

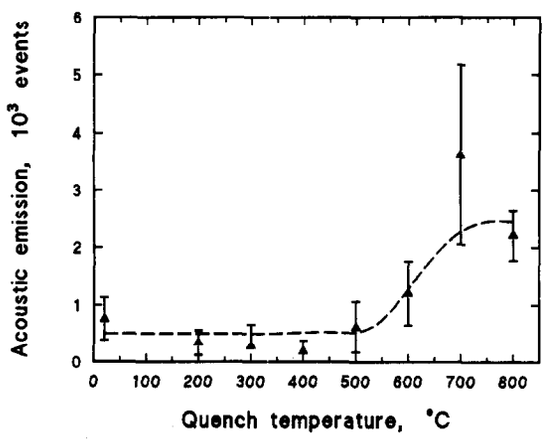

Fig. 5. Cumulative acoustic emission event count during flexural fracture tests on quenched samples of the Nextel/silica–zirconia CMCs.

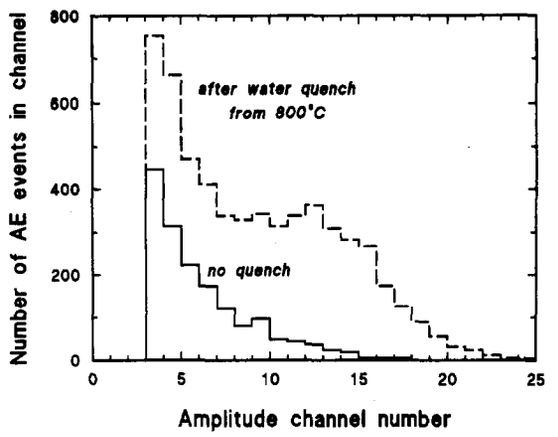

Fig. 6. Acoustic emission amplitude distributions for Nextel/silica–zirconia CMC samples tested to failure in flexure in the as-received condition and after quenching from 800°C.

5 Discussion

It is apparent from Fig. 3 that although, in the quench temperature range below 500°C, the mean strength and toughness values both begin to decline, somewhat more gently than the stiffness values, all of these reductions are still within the overall spread of experimental results and the real effect of thermal shock is more obviously manifested as a step reduction in all three properties at some quenching temperature between 500 and 550°C. Beyond this temperature all three properties remain constant, again within the scatter of the results.

The basic Kingery model[4] for an infinitely rapid quench of a ceramic body gives the maximum temperature difference, ΔT_c, which a material can withstand before the fracture stress, σ_f, is reached as

$$\Delta T_c = (R^I) = \frac{\sigma_f (1 - \nu)}{E\alpha} \quad (2)$$

Since we have no experimental results for the thermal conductivity of our composites, it is not possible to refine the model to account for finite quenching rates and finite sample geometry, but eqn 1 may be used to evaluate the results in Fig. 3, at least to a first approximation. The theoretical value of ΔT_c for a composite exhibiting the properties that would have been predicted from the basic characteristics of the matrix and fibres would have been of the order of 1200°C, assuming a mean value of α of $5{\cdot}5 \times 10^{-6}(°C)^{-1}$. As we have seen, however, the real strength of the composite is a fraction of the predicted value, and if we insert the actual experimental values from Table 1, together with a mean value of α of $4 \times 10^{-6}(°C)^{-1}$, we find that the predicted ΔT_c is about 375°C. The problem is, of course, recursive since, as we showed earlier, the actual value of α, and also its mean value over the predicted quenching range, are themselves functions of that temperature range, and these approximate values of α and ΔT_c must be obtained by successive approximations. The observation that slower cooling does not produce a change in strength implies that the second thermal shock parameter

$$R^{II} = \frac{k\sigma_f (1 - \nu)}{E\alpha} \quad (3)$$

is not significant, i.e. the conductivity, k, is not a contributor to the grading of the materials — they are susceptible only to large, rapid quenches.

It is interesting to note that a very limited number of flexural tests carried out on samples cut transverse to the fibre axis gave values of 6 GPa and 13 MPa, respectively, for the modulus and strength, and these values generate a slightly higher calculated value of ΔT_c, about 406°C, but both predicted values are 150°C or more below the clearly defined experimental value which is between 500 and 550°C.

It appears, therefore, that despite the apparently large loss in strength of the reinforcing fibres during the fabrication process, their presence remains beneficial in increasing the resistance of the material to thermal shock. We note that unreinforced freeze-gelled material has a failure strength of about 20–30 MPa and a work of fracture of 0·05–0·1 kJm^{-2}. Thus, although our experimental material is relatively weak by comparison with high-performance CMCs, it was significantly better than the unreinforced material.

The more complete Hasselmann model[5] predicts that for thermal shocks of severity less than ΔT_c the strength remains unaffected because insufficient strain energy is available to cause propagation of a number of existing flaws (which are assumed to be of a uniform size). The fibres are likely to contribute to the increase of energy required to propagate all of these flaws. When the temperature difference exceeds the critical value, the strength (and, as shown by Fig. 1, any other mechanical property associated with strength as normally defined) falls because a significant proportion of the family of pre-existing cracks has grown as a result of the thermal shock. The process of propagation of these larger cracks is stable, however, and no further drop in strength is expected with further increase in the quenching temperature interval until a second critical temperature difference, $\Delta T_c'$, is reached when the cracks present in the quenched body have become large enough to propagate in quasi-static fashion, with corresponding further decrease in strength as ΔT increases further. It can be seen from Fig. 3, however, that this higher critical temperature interval has not been reached by the time the thermal shock experiments were discontinued at 800°C, above which structural changes in the material would be expected.

The acoustic emission response of the materials in the as-manufactured and quenched states appears to be quite different. During the early stages of loading, samples quenched from above 500°C emit fewer acoustic emissions than un-quenched samples, but as failure approaches the event emission rate increases more rapidly so that, overall, quenched samples produce more events to failure. It has also been shown that a mid-range amplitude peak develops as failure approaches, indicating the possibility of the onset of a micro-failure process that is different from that which occurs normally in un-quenched material. The likelihood

is that this mechanism is the propagation of pre-existing cracks formed or extended by the thermal shock treatment. It appears, then, that cracks are propagating subcritically during thermal shock, presumably from existing defects (pores, perhaps, or reaction damage sites on fibres). During loading of quenched samples, a higher level of strain is then required to cause further propagation and stimulate AE. As failure approaches, however, the number of enlarged cracks results in more AE. The marked decline in composite strength caused by quenching suggests that the thermal shock process must also be causing further damage to the fibres, presumably as a result of the matrix cracks propagating through the fibres as a consequence of the strong interfacial bond.

6 Conclusions

(1) Ceramic-matrix composites consisting of a silica–zirconia matrix reinforced by continuous Nextel mullite fibres have been manufactured by a sol–gel route incorporating freeze-gelation and subjected to thermal shock by water quenching from temperatures up to 800°C.

(2) Nextel alumino-silicate fibres are unsuited to direct inclusion in freeze-gelled ceramic matrix composites, probably because of degradation of the fibres during the desizing and filament winding processes. The lack of appropriate low-cost ceramic reinforcing fibres and the requirement for interface control through the application of interfacial layers is nothing new in the field of CMCs.

(3) Despite 2 above, comparison of reinforced and unreinforced freeze-gelled material shows that the Nextel fibres provide significant reinforcement of the matrix and improvements in the thermal shock resistance. Nextel-fibre-reinforced silica/zirconia CMCs are essentially unaffected by water quenching from temperatures up to 550°C. Beyond this critical value there is a step reduction of strength and modulus to between 50 and 60% of virgin properties.

(4) The changes in mechanical behaviour are accompanied by significant modifications of the acoustic emission response of the materials during post-quench three-point flexural testing. A lower initial event rate during load application gives way to a much higher event rate (and more events in total) at failure. A change to a bi-modal amplitude distribution near failure gives further credence to the hypothesis that thermal shock (beyond a critical value) causes the propagation of probably pre-existing flaws to a longer but stable value. A further, and significantly higher second critical level of thermal shock is then required to cause additional propagation of the flaws and a further reduction in properties. In other words, we believe that our continuous fibre reinforced materials behave in the manner proposed by Hasselmann. We note that earlier work of a similar nature on a freeze-cast short-fibre-reinforced CMC showed that this material also obeyed the Hasselmann model.[6]

(5) Quenching from above the critical temperature results in a significant (but not catastrophic) decline in strength which is not altered by further increasing the quenching temperature. The Hasselmann quenching cracks clearly do not therefore propagate from one side of the sample to the other.

Acknowledgement

This work was carried out as part of a wider program of research on the sol–gel processing of CMC shapes with the financial support of the ACME Directorate of SERC. The authors are grateful for this support and for the encouragement of the Directorate. Sadly, Dr Richard Russell-Floyd, who was a major source of inspiration in this work, died shortly after this paper was submitted for publication.

References

1. Russell-Floyd, R., Harris, B., Jones, R. W., Cooke, R. G., Wang, T. H., Laurie, J. & Hammett, F. W., *Br. Ceram Trans*, **92** (1993) 8–12.
2. Russell-Floyd, R. S., Harris, B., Cooke, R. G., Wang, T. H., Laurie, J., Hammett, F. W. & Jones, R. W., *Journal of the American Ceramic Society*, **76**(10) (1993) 2635–43.
3. Chant, J. M. (1994). University of Bath, private communication of unpublished results.
4. Kingery, W. D., *J. Am. Ceram. Soc.*, **1** (1955) 3–15.
5. Hasselmann, D. P. H., *J. Am. Ceram. Soc.*, **52** (1969) 600–4.
6. Russell-Floyd, R. S., Johnson, R., Cooke, R. G. & Harris, B., *Advanced Composites Letters*, **2** (1993) 57–60.